Cryogenic far-infrared laser absorptivity measurements of the Herschel Space Observatory telescope mirror coatings

Jacqueline Fischer, Tjeerd Klaassen, Niels Hovenier, Gerd Jakob, Albrecht Poglitsch, and Oren Sternberg

Far-infrared laser calorimetry was used to measure the absorptivity, and thus the emissivity, of aluminum-coated silicon carbide mirror samples produced during the coating qualification run of the Herschel Space Observatory telescope to be launched by the European Space Agency in 2007. The samples were measured at 77 K to simulate the operating temperature of the telescope in its planned orbit about the second Lagrangian point, L_2, of the Earth–Sun system. Together, the telescope's equilibrium temperature in space and the emissivity of the mirror surfaces will determine the far-infrared–submillimeter background and thus the sensitivity of two of the three astronomical instruments aboard the observatory if stray-light levels can be kept low relative to the mirror emission. Absorptivities of both clean and dust-contaminated samples were measured at 70, 118, 184, and 496 μm. Theoretical fits to the data predict absorptivities of 0.2–0.4% for the clean sample and 0.2–0.8% for the dusty sample, over the spectral range of the Herschel Space Observatory instruments.

OCIS codes: 350.6090, 350.5340, 110.3080, 110.6770, 110.4280, 160.4760.

1. Introduction

For passively cooled telescopes such as the European Space Agency's (ESA's) Herschel 3.5-m silicon carbide (SiC) telescope[1,2] to be launched in 2007 aboard an Ariane 5 rocket to orbit the Earth–Sun second Lagrangian point, L_2, the signal from the thermal self-emission of the Cassegrain telescope's reflecting surfaces is expected to be the dominant source of noise for two of the three observatory instruments. Thermal models of the telescope–spacecraft system predict an equilibrium operating telescope temperature in the range 70–90 K. Both the Photodetector Array Camera & Spectrometer[3] (PACS) and the Spectral and Photometric Imaging Receiver[4] (SPIRE), which together provide both imaging and moderate resolution ($\lambda/\Delta\lambda$ 100–2000) spectroscopy over the 55–670-μm spectral range, are expected to be background limited by the thermal self-emission of the telescope's reflecting mirrors. To estimate the sensitivity of these instruments in orbit and the background flux on their detectors and to determine to what extent further reduction of stray light originating from thermal emission from payload objects is necessary, we have carried out a set of measurements designed to estimate the expected emissivity of the mirror surfaces in orbit in the far-infrared–submillimeter spectral range.

2. Experiment Concept

According to Kirchhoff's law,[5] for equilibrium conditions the fraction of blackbody radiation emitted by the surface of an object at a given temperature and wavelength, i.e., its emissivity ε, is equal to the fraction that it absorbs at the same temperature and wavelength, i.e., its absorptivity α. This applies to total, spectral, directional, and polarization quantities. Thus one can indirectly measure the emissivity of a surface by calorimetrically measuring the fraction of radiation that the surface absorbs at a

J. Fischer (jackie.fischer@nrl.navy.mil) and O. Sternberg are with the Remote Sensing Division, Naval Research Laboratory, Code 7213, Washington, D.C. 20375. T. O. Klaassen and J. N. Hovenier are with the Faculty of Applied Sciences, Delft University of Technology, P.O. Box 5046, 2600 GA Delft, The Netherlands. G. Jakob and A. Poglitsch are with the Max-Planck-Institut für Extraterrestrische Physik, Postfach 1603, D-85740, Garching, Germany.

Received 1 December 2003; revised manuscript received 12 April 2004; accepted 19 April 2004.

0003-6935/04/193765-07$15.00/0

given wavelength. To do this we developed an experimental procedure in which Herschel Telescope mirror samples are weakly coupled to a thermal bath and then illuminated by far-infrared (FIR) radiation of known wavelength and power P_0 until a stable sample temperature is reached. The resultant small temperature increase ΔT is recorded through a temperature sensor, which is glued to the back side of the sample. Subsequently the FIR radiation is blocked and the sample is electrically heated by a resistor, which is also glued to the back side of the sample. The heating current is then adjusted until the sample reaches equilibrium at the same temperature that was recorded during laser illumination, thereby heating the sample with power $P_H = I_H V_H$, where I_H and V_H are the heater's current and voltage, respectively. As the conductivity of SiC is high, the heat is quickly distributed across the sample, and thus the electrical and radiative heat input required to reach the same reading of the temperature sensor are equal; i.e., the electrical heating power P_H is equal to the absorbed FIR power, P_{abs}. Finally, if the incoming power P_0 can be experimentally determined, the absorptivity α and thus the emissivity ε at a given laser wavelength can be ascertained:

$$\varepsilon = \alpha = P_{\mathrm{abs}}/P_0 = P_H/P_0. \quad (1)$$

For opaque coatings the reflectivity R is $1 - \alpha$, so formally one can measure α by measuring R,[6] which is often an easier quantity to measure. However, for coatings with high reflectivity and small absorptivity, say, $R > 0.99$ and $\alpha < 0.01$, the required accuracy in the determination of R, of the order of 0.1%, is prohibitively difficult to achieve. Alternatively, one can measure the emissivity of a sample by comparing the thermal emission with that of a reference surface.[7] To avoid the need for special filters at each wavelength, and because of the lack of a suitable reference surface, we instead chose absorption calorimetry.

3. Experimental Configuration and Calibration

A. Sample Preparation

To represent the Herschel Space Observatory telescope most accurately, SiC sample substrates were prepared by Boostec Industries (France) and polished with the same surface roughness as the Herschel Telescope (<30 nm rms) by Opteon, Ltd. (Finland) for the European Aeronautic Defense and Space (EADS)–Astrium Company (France). The samples were cut and ground to dimensions of 14 mm × 14 mm × 0.5 mm to minimize their heat capacity while ensuring that the beam could be focused onto the sample even at the longest measurement wavelength. The samples were coated with aluminum and a thin protective layer of Plasil, a form of SiO_2 developed by Leybold Optics (Germany) during the qualification Herschel mirror coating run at Calar Alto Astronomical Observatory in Spain. Because the samples were placed at different positions in the coating chamber, different coating thicknesses d were deposited for each sample. For sample 1, d(aluminum) = 400 nm and d(Plasil) = 25 nm, and for sample 2, d(aluminum) = 300 nm and d(Plasil) = 7 nm. Measurements were made of the two samples with the largest thickness differences.

A third set of measurements of sample 2 was made after the sample had been contaminated with dust at a level of 5000 ± 50 areal parts in 10^6 (ppm).[8] Before their contamination the clean samples were inspected with bright illumination, and microscope cleanliness and particle counting tests were performed; the samples were found to be free of gross defects and had minimal contamination, with no particles larger than 5 μm. Dust for the contamination was collected from a class 100,000 clean room at the European Space Research and Technology Centre (ESTEC) test center. This type of dust was chosen to be representative of what might fall upon the Herschel Telescope prior to and during launch, although the exact chemical composition and size distribution of clean room dust may be variable. A clean paintbrush was used to deposit the dust onto the sample to a level of 15,000 ppm. Subsequently the level was adjusted to 5000 ppm with a soft helium-gas flow. The particle count was rechecked after the sample was vertically positioned in a vacuum chamber at 10^{-4}-Pa pressure and again after completion of the absorptivity measurements in the cryostat. After the cold measurements the average particle count measured on four plates in scattered light by a particle-fallout meter was found to be 5000 ± 50 ppm. Particle count and size measurements were also carried out at six positions with a total area of 60 mm^2, before and after the absorptivity measurements. The results were found to be roughly similar at the six positions and before and after the measurements. The particle size and areal distribution from these measurements are listed in Table 1. The counts are averages of values obtained before and after the absorptivity measurements.

Table 1. Number and Size Distribution of Dust Particles[a]

Particle size (μm)	Number of Particles in 60 mm^2	Surface Area in 60 mm^2 ($\times 10^4$ μm^2)	Dust Contamination (ppm)
5–15	286	2.80	467
15–25	187	6.22	1037
25–50	76	9.33	1554
50–100	26	12.50	2083
>100	0		
Total			5141

[a]Source: Ref. 8.

B. Sample Housing and Sample Thermal Connection to the 77-K Bath

Samples prepared during the Herschel Telescope coating qualification run were mounted in a sample housing that was mounted on the cold plate of a Dewar filled with liquid nitrogen at 77 K. Figure 1 is a photograph of the sample carrier in the sample

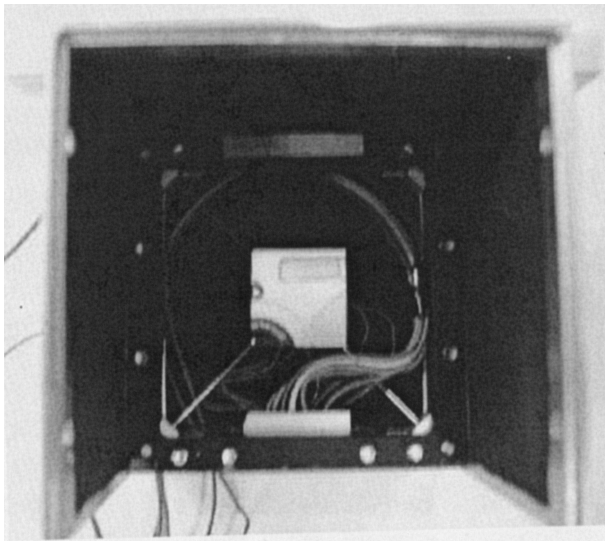

Fig. 1. Photograph of a sample and a sample carrier mounted in the sample housing.

housing. The sample carrier and the inner surfaces of the box were coated with black paint, and the wires and electrical connections to the sample were baffled by aluminum tape (not shown in Fig. 1). The samples were held by four steel wires of 200-μm diameter and length of ~23 mm, which were attached with screws to the rectangular carrier. The carrier was screwed to the box, and the sample box was directly screwed to the 77-K cold plate of the cryostat. The choice of the exact value of the thermal coupling of the sample to the 77-K bath, G, was a trade-off between the desire to reach a large temperature increase and a small thermal time constant. The thermal time constant τ is C/G, where C is the heat capacity of the sample, and the temperature increase $\Delta T \propto P_{abs}/G$. The electrical connection of the heater (two wires) and the temperature sensor (four wires) was accomplished with six constantan wires of 75-μm diameter and ~40-mm length. These parameters were chosen to yield a thermal time constant of minutes and to be such that the contribution of the constantan wires to the thermal coupling would be small compared with that of the four steel wires. Experimentally we found that thermal time constant τ was of the order of 10 min, during which time the laser was stable and the temperature increase ΔT was large enough (≥0.1 K) to be measured easily.

C. Optical Configuration

The measurements were performed at the Delft University of Technology in The Netherlands, which provided an Edinburgh Instruments Ltd. Model 295 CO_2-pumped FIR laser. To cover most of the spectral range of the Herschel Space Observatory suite of instruments we chose four strong lines for the measurements: the 70- and 118-μm lines of CH_3OH (methanol), a 184-μm line of CH_2F_2, and a 496-μm line of CH_3F. Figure 2 is a schematic drawing of the optical setup of the FIR laser absorption measurements, and Figs. 3 and 4 are photographs of the optical setup and the cryostat cold plate. A 12-μm-thick Mylar beam splitter reflected a small fraction of the laser power to a pyroelectric monitor to record any change of the incoming laser power. A polyethylene lens focused the laser beam through the polyethylene cryostat window onto the sample, which was tilted at an angle of 14° with respect to the laser beam. This configuration directed the reflected beam onto an absorptive screen located in front of the cryostat window. This screen, which comprised an aluminum substrate coated with an absorptive mixture[9] of 1-mm silicon carbide grains and black Stycast 2850 FT (a low-temperature, two-component resin manufactured by Emerson and Cuming, 46 Manning Road, Billerica, Massachusetts), absorbed 95% of the radiation reflected from the sample. To absorb any radiation spilling over the edge of the sample, an identical absorbing screen was mounted onto the rear wall of the sample housing. A flip mirror in front of the cryostat was used to send light periodically to a second pyroelectric detector located at the same distance from the lens as the sample to monitor the position and the beam profile of the focused beam at the sample. Horizontal and vertical $1/e^2$ beam diameters measured with the monitor were 5.7–7.0 mm at wavelengths of 70, 118, and 184 μm and 12–14 mm at 496 μm. Before and after the FIR irradiation of the sample, a slide-in mirror, also in front of the cryostat window, was used to direct the light to a Scientech 372-380101 powermeter–calorimeter to

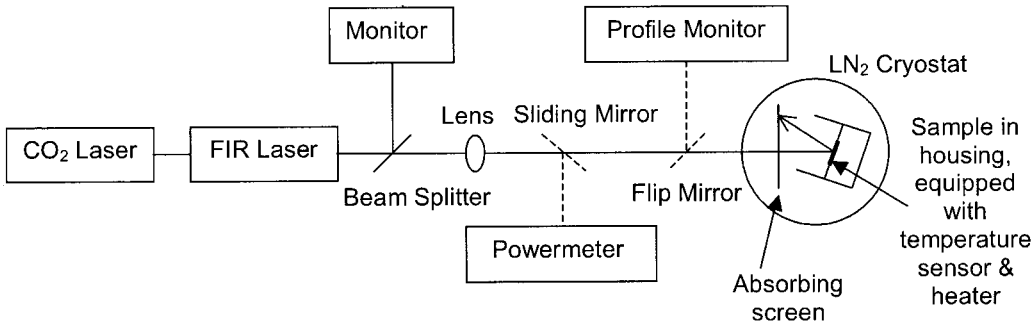

Fig. 2. Schematic drawing of the optical configuration used for the measurements. Sliding and flip mirrors are inserted into the beam for power calibration and beam profile verification, respectively, as shown.

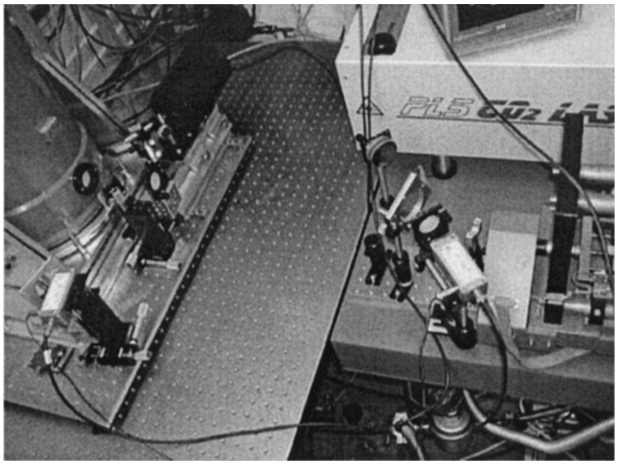

Fig. 3. Photograph of the optical layout, including the front end of the FIR laser at the extreme right.

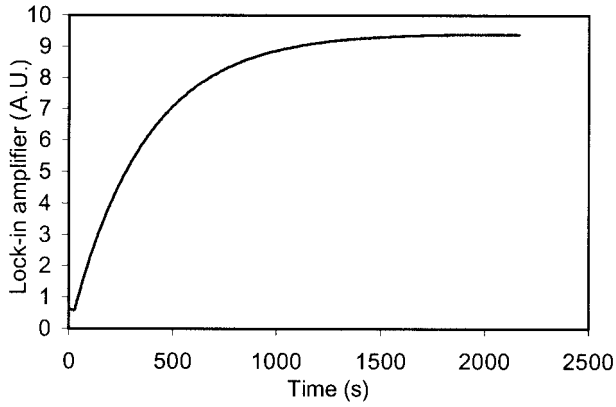

Fig. 5. Typical heating curve for a clean mirror sample at 77 K. The increase in lock-in amplifier signal corresponds to a temperature rise of ~300 mK with a thermal time constant of ~7 min and has a noise level of ~0.6 mK (rms).

measure the laser power incident onto the window of the cryostat. (The determination of the absolute calibration of this powermeter at the laser line wavelengths is described in Subsection 3.E below.)

D. Electrical Configuration

The temperature increase in the sample that resulted from either FIR illumination or electrical heating with a thin-film metal resistor (R_H = 470 Ω, with negligible temperature dependence) was measured with a Pt-1000 temperature sensor at the back side of the sample. A Pt-1000 temperature sensor was also mounted on the sample housing, which was in good thermal contact with the cryostat cold plate. An ac Wheatstone bridge circuit was used to measure the temperature of the sample. In this circuit the ratio of a pair of 10-kΩ resistors at ambient temperature, one fixed and one adjustable, was balanced with the ratio of the two Pt-1000 cold resistances, each approximately equal to 200 Ω at liquid-nitrogen temperature. The current across the bridge was measured with a lock-in amplifier and set to zero, providing a precise method by which to match the electrical heating power to that of the laser illumination. Because the temperature difference between the two Pt-1000 sensors was measured with this circuit, slow variations in the cold plate temperature, which were due, for instance, to changes in the ambient pressure, did not affect the results. With this method a rms noise level of ~0.6 mK was achieved, producing a significantly better signal-to-noise ratio than what was achieved with a four-point direct resistance measurement in an earlier calorimetric experiment.[9] An example of a typical heating curve is shown in Fig. 5.

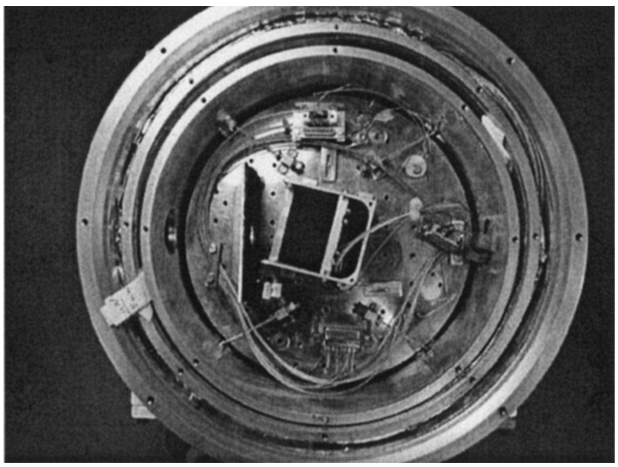

Fig. 4. Photograph of the open cryostat cold plate and sample housing. The laser beam enters through the cryostat window (left), passes through the aperture in the absorbing screen, and is reflected by the tilted sample back onto the absorbing screen.

E. Power Calibration

Critical to the concept of this technique of measuring the absorptivity of a sample is knowledge of the incident far-IR radiation power. During measurement of the sample, a Scientech 380101 UV/NIR volume-absorbing calorimeter interfaced to a Scientech 372 powermeter was used to monitor and record the level of laser power incident onto the cryostat window. The absolute far-IR–submillimeter calibration of this powermeter was accomplished by comparison of the Scientech reading with the reading of an absolute powermeter that was newly developed for this purpose[10] for each of the laser wavelengths used for the sample measurements. The new powermeter uses a calorimetric concept and a Wheatstone bridge setup similar to that used for the determination of the absorption of our samples but in this case it used the known room-temperature FIR absorption of the absorptive SiC 1-mm grain–Stycast mixture.[9] The transmission of the polyethylene cryostat window was measured independently from the drop in power that appeared on the Scientech calorimeter as a result of the insertion of the window into the laser beam. The effect of differences in water vapor absorption that are due to the slightly different path lengths to the sample and to the Scientech calorim-

Table 2. Absorptivities (%) of the Three Measured Samples at 77 K

Sample Number and Characteristics	Wavelength (μm)			
	70	118	184	496
1; 300-nm Al, 7-nm Plasil	0.31 ± 0.04	0.32 ± 0.04	0.27 ± 0.04	0.33 ± 0.08–0.17
2; 400-nm Al, 25-nm Plasil	0.39 ± 0.05	0.32 ± 0.04	0.28 ± 0.04	0.36 ± 0.09–0.18
3; sample 2 with 5000 ± 50 ppm dust	0.79 ± 0.11	0.54 ± 0.08	0.39 ± 0.05	0.23 ± 0.06–0.12

eter was measured and used to correct the calorimeter's power readings.

4. Measurements and Uncertainties

Measurements of the heater power that produced the same temperature increase as the laser power absorbed by the mirror and of the power measured by the Scientech powermeter were made with the beam centered on the sample. To ensure that this value was representative, we made a number of measurements at beam positions around the sample center. We varied the position of the beam by moving the focusing lens in transverse directions and monitored it by using the second pyroelectric detector. Near the edges of the sample, clear changes in the magnitude of the heating were observed. Intentional spillover of the beam was found to lead to a strong increase in sample heating, because some of the spillover radiation hit the curved edge of the sample housing, which was not covered by the flat absorbing screen behind the sample (see Fig. 4). As the black paint on the inside of the housing is not a good absorber at these wavelengths, a considerable fraction of that radiation was directly reflected onto the highly absorbing back side of the sample, causing this increased heating.

The systematic uncertainties in the absorptivity measurements are due to errors in the determination of window transmission, absolute powermeter sensor absorption coefficient, path-length difference corrections, electrical power absorbed, and signal ratio of the absolute powermeter to the Scientech powermeter. We estimate these errors to be ±5%, ±5%, ±5%, ±5%, and ±10%, respectively, at 70, 118, and 184 μm. Error propagation leads to total uncertainties of ±14%. At 496 μm, the larger size of the beam diameter is thought to lead to a small amount of spillage of the laser power over the edge of the sample, with subsequent scattering leading to nonnegligible absorption on the back side of the sample and consequently to systematic errors of approximately +25% and −50% in the determination of the absorptivity.

The absorptivity values and their calibration uncertainties are given in Table 2. They are based on the weighted mean values of the ratio of the electrical heating power, P_H, to the power reading on the Scientech powermeter measured at a small number of positions in the central region of the sample. There is no statistically significant difference between the measured values of the two clean samples, despite their different thicknesses of aluminum and Plasil layers. Inasmuch as the skin depth of aluminum at 77 K is more than an order of magnitude smaller than the thickness of the aluminum layer on both samples, no laser radiation is expected to reach the SiC substrate for either sample. Thus the similarity in the absorptivity of the two clean samples suggests that the absorption in the Plasil layer is less than our measurement uncertainties, i.e., <0.10%. To check for a strong temperature dependence of the emissivity in this temperature range we took one measurement at each wavelength at 66 K while the liquid-nitrogen bath was pumped for samples 1 and 2. No statistically significant differences were observed.

5. Model Fits to the Measurements

The averages of the absorptivity measurements of the two clean samples are plotted in Fig. 6. The measured absorptivity values are 0.1–0.2% higher than those expected for a pure aluminum mirror based on the Hagen–Rubens formula[11] and the dc resistivity of aluminum[12] at 77 K (0.23×10^{-8} Ω m; dotted curve in Fig. 6). With resistivity taken as a free parameter in the Hagen–Rubens formula, the best fit to the data (we used the 70-, 118-, and 184- but not the 496-μm data because of the larger uncertainty of the last-named value) yielded a resistivity of 0.85×10^{-8} Ω m,

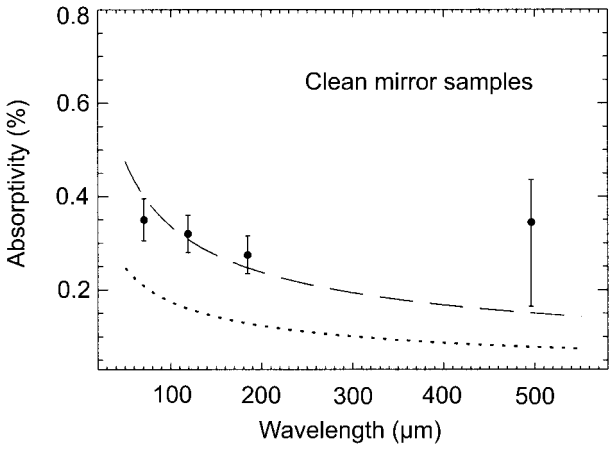

Fig. 6. Measurements and estimated uncertainties for the clean mirror samples. Because there were no significant differences in the measurements for the two clean samples, the average values are shown. The dotted curve is the absorptivity expected for a pure aluminum mirror based on the Hagen–Rubens[11] formula and the resistivity[12] of aluminum at 77 K. The dashed curve shows the best fit to the data, excluding the measurement at 496 μm, with resistivity taken as a free parameter (see text).

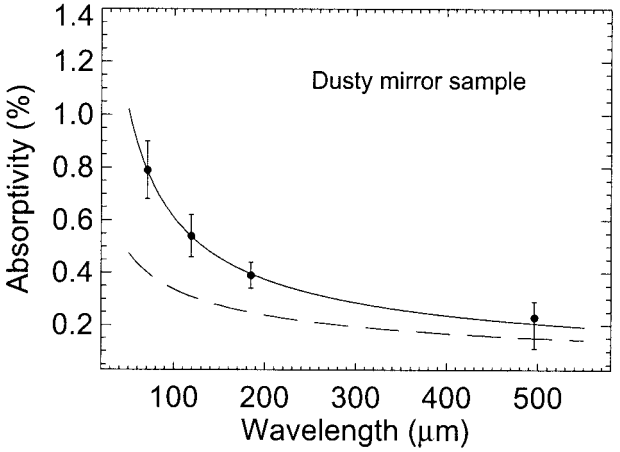

Fig. 7. Measurements and estimated uncertainties for the dusty mirror sample. The dashed curve shows the best fit to the clean mirror sample (see Fig. 6), and the solid curve shows the best fit to the dusty mirror data (excluding the measurement at 496 μm) using the sum of the clean mirror fit and a λ^{-1} absorptivity dependence for the dust (see text).

3.7 times higher than the dc value (dashed curve in Fig. 6). Discrepancies at this level are commonly observed and are attributed to surface roughness and surface preparation issues and to the complex and frequency-dependent nature of a metal's resistivity.[6] In particular, we investigated the importance of the small holes that were observed on the surfaces of the Herschel mirrors (100 holes/mm^2, radii, ~2 μm) and were due to the preparation of the SiC substrate by electromagnetic field simulation software, and we found no significant effect caused by the presence of the holes. The fit fell within the estimated errors except at 496 μm; we attribute this discrepancy to the difficulty of estimating systematic uncertainties.

The measurements and uncertainties are plotted in Fig. 7 for the dusty mirror sample. These values, including the highest dust absorptivity value of 0.004 at 70 μm, are consistent to within the measurement uncertainties with the dust particle surface's areal density of 0.005, because peak absorption efficiencies as high as 2 are found for spherical dust particles.[13] The spectral dependence of the emissivity of dust particles for wavelengths greater than the particle size is expected to be of the form $\lambda^{-\beta}$, where $1 \leq \beta \leq 2$.[14] The best fit to the absorptivity of the clean sample measurements (dashed curves in Figs. 6 and 7) was added to an absorptivity proportional to $\lambda^{-\beta}$ for $\beta = 1, 1.5, 2$. The best fit to this part of the spectrum for the dusty sample (solid curve in Fig. 7) obtained with the proportionality constant as a free parameter was found for $\beta = 1$; specifically,

$$\alpha = 0.0336\lambda^{-0.5} + 0.273\lambda^{-1}. \quad (2)$$

Again, the 496-μm measurement was not used to obtain the fit, but it is consistent with the fit.

6. Implications for the Herschel Space Observatory

The measurements reported here provide information that is important to the final design of the Herschel Telescope's structure, its surroundings, and its baffle system. The emissivity values measured for all samples are significantly lower than the contractually specified values for the telescope mirrors, i.e., 1.5% per mirror. To ensure that the full benefit of the low emissivity and the cold telescope temperature achieved by the design of the telescope and its surroundings are utilized, extreme care will need to be taken to reduce the levels of stray light reaching the instrument focal plane array detectors from warm or effectively high-emissivity payload objects such as the sunshade and the cryostat cover and surrounding cavity. Inasmuch as the ideal conductance of the bolometer arrays for achievement of the greatest array sensitivity depends on the level of the operating background radiation, and because the conductance can be modified during an etching step in a relatively late stage of the array fabrication, the emissivity measurement values presented here have additional practical importance. These results will also provide important input to observing time-estimation calculations that will determine the types of observing programs that will be feasible with this potentially powerful new observatory. Similar measurements near the peak of the thermal emission range would help to improve the accuracy of predictions of the equilibrium temperature of the telescope.

We gratefully acknowledge suggestions made by Herschel project scientist Göran Pilbratt and by Pierre Olivier (ESA/ESTEC), helpful discussions on dust absorption properties with Chris Dudley (U.S. Naval Research Laboratory), mirror samples supplied by Dominique Pierot (EADS–Astrium, France), and sample contamination and characterization by Olivier Schmeitzky and Mark van Eesbeck (ESA–ESTEC). We thank Thomas Passvogel and Daniel de Chambure for making available partial funding of these measurements from the ESA Herschel–Planck Project office. J. Fischer and O. Sternberg (National Research Council Research Associate) acknowledge support from the U.S. Office of Naval Research and the National Aeronautics and Space Administration's Herschel Project Office at the Jet Propulsion Laboratory, California Institute of Technology.

References

1. E. Sein, Y. Toulemont, F. Safa, M. Duran, P. Deny, D. de Chambure, T. Passvogel, and G. Pilbratt, "A Φ 3.5 M SiC telescope for Herschel mission," in *IR Space Telescopes and Instruments*, J. Mather, ed., Proc. SPIE **4850,** 606–618 (2003).
2. G. Pilbratt, "Herschel Space Observatory mission overview," in *IR Space Telescopes and Instruments*, J. Mather, ed., Proc. SPIE **4850,** 586–597 (2003).
3. A. Poglitsch, C. Waelkens, and N. Geis, "The Photodetector Array Camera & Spectrometer (PACS) for the Herschel Space Observatory," in *IR Space Telescopes and Instruments*, J. Mather, ed., Proc. SPIE **4850,** 662–673 (2003).
4. M. Griffin, B. Swinyard, and L. Vigroux, "SPIRE—Herschel's submillimetre camera and spectrometer," in *IR Space Tele-*

scopes and Instruments, J. Mather, ed., Proc. SPIE **4850,** 686–696 (2003).
5. W. L. Wolfe, "Radiation theory," in *Sources of Radiation*, G. J. Zissis, ed., Vol. 1 of The Infrared & Electro-Optical Systems Handbook, J. S. Accetta and D. L. Shumaker, eds. (ERIM, Ann Arbor, Mich., 1993), pp. 1–48.
6. A. J. Gatesman, R. H. Giles, and J. Waldman, "High-precision reflectometer for submillimeter wavelengths," J. Opt. Soc. Am. B **12,** 212–219 (1995).
7. J. J. Bock, M. K. Parikh, M. L. Fischer, and A. E. Lange, "Emissivity measurements of reflective surfaces at near-millimeter wavelengths," Appl. Opt. **34,** 4812–4816 (1995).
8. O. Schmeitzky, "Particle contamination simulation on SCI-sample-wafer Herschel–Planck project," internal rep. TOS-QMC 2003/134 (European Space Research and Technology Center, Noordwijk, The Netherlands, 2003).
9. T. O. Klaassen, J. H. Blok, J. N. Hovenier, G. Jakob, D. Rosenthal, and K. J. Wildeman, "Scattering of sub-millimeter radiation from rough surfaces: absorbers and diffuse reflectors for HIFI and PACS," in *IR Space Telescopes and Instruments*, J. Mather, ed., Proc. SPIE **4850,** 788–796 (2003).
10. T. O. Klaassen, J. N. Hovenier, J. Fischer, G. Jakob, A. Poglitsch, and O. Sternberg, "THz calorimetry: an absolute power meter for terahertz radiation and the absorptivity of the Herschel Space Observatory telescope mirror coating," in *Terahertz and Gigahertz Electronics and Photonics III*, R. J. Hwu, ed., Proc. SPIE **5354** (to be published).
11. M. Born and E. Wolf, *Principles of Optics*, 6th ed. (Pergamon, Oxford, 1986).
12. G. W. C. Kaye and T. H. Laby, *Tables of Physical and Chemical Constants*, 16th ed. (Longman, Essex, UK, 1995).
13. H. C. van de Hulst, *Light Scattering by Small Particles* (Dover, New York, 1957).
14. B. T. Draine and H. M. Lee, "Optical properties of interstellar graphite and silicate grains," Astrophys. J. **285,** 89–108 (1984).